

SC651 : Assignment 1

Adityaya Dhande 210070005

1 Numerical integrators

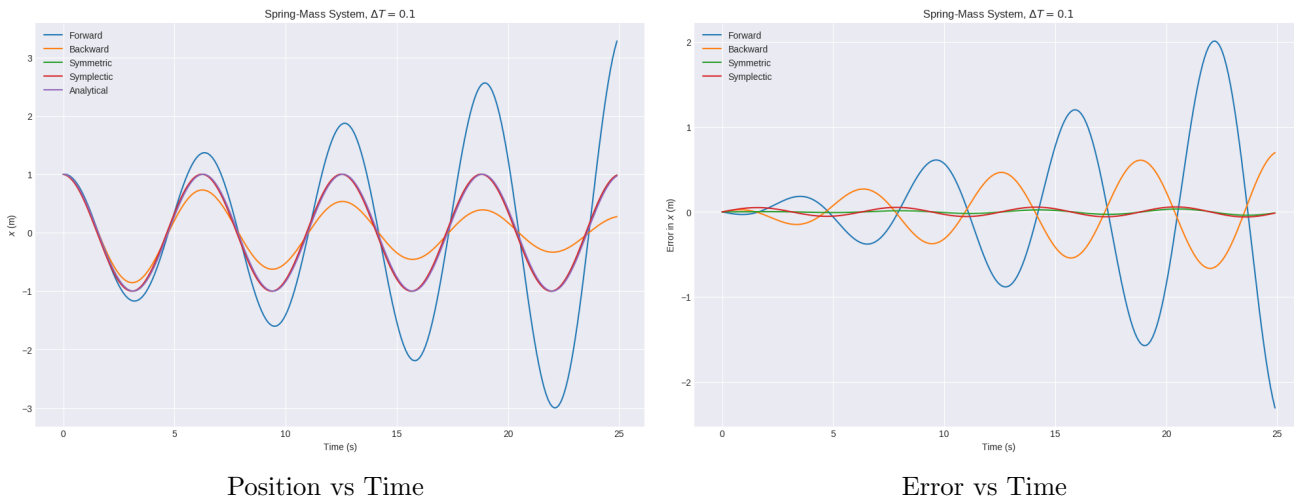
I have simulated the spring-mass system without a damper to better study the performances of different numerical integrators. I implemented the four different numerical integration methods – **Forward Euler**, **Backward Euler**, **Symmetric Euler**, **Symplectic Euler** for both the Spring-Mass and Vertical Pendulum system. I also evaluated the analytical solution for the Spring-Mass system and used it to analyse the performances of the different numerical methods.

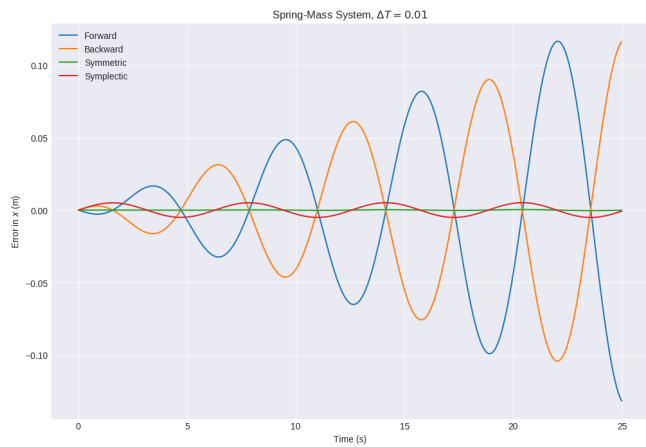
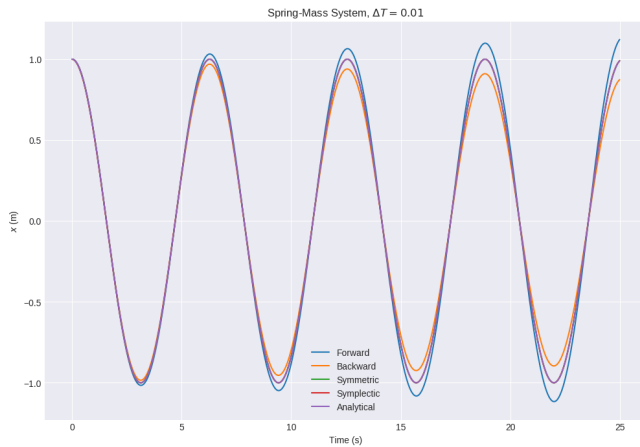
Spring-Mass system : Analysis with varying time-steps

Variation of **absolute average error (in metres)** with ΔT

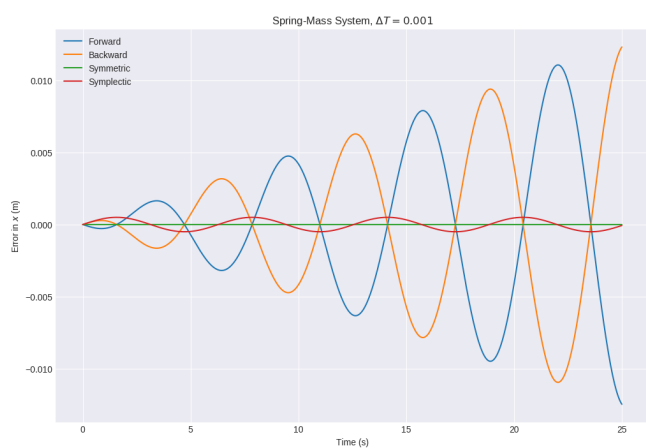
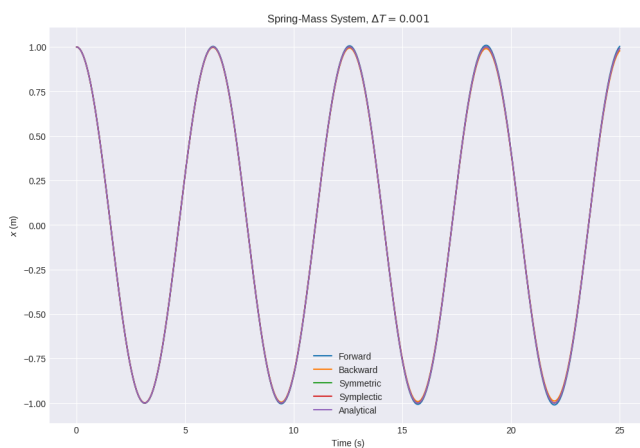
$\Delta T(s)$	Forward	Backward	Symmetric	Symplectic
0.1	0.6153	0.2703	0.0134	0.0353
0.01	0.0412	0.0379	0.0001	0.0032
0.001	0.0040	0.0039	1.34e-6	0.0003

The solution obtained using **Forward Euler** grows unbounded and the solution obtained using **Backward Euler** dies down over time, as opposed to the original solution which is sinusoidal and does not grow unbounded with time. The performance of **Symmetric Euler** and **Symplectic Euler** is significantly better. The error of Symplectic Euler solution is initially higher than that of Symmetric Euler, but the error of Symmetric Euler solution grows at a faster rate.

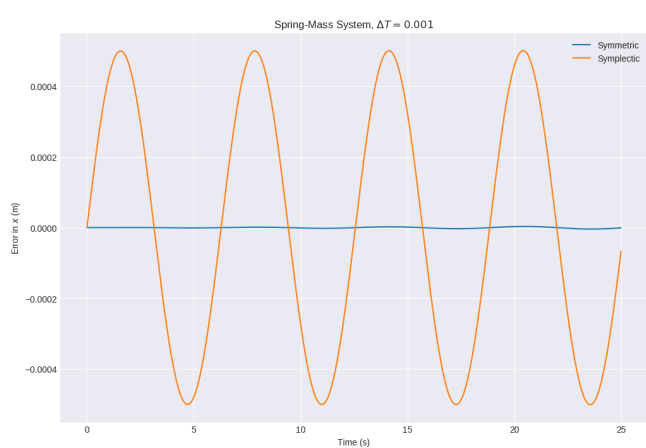
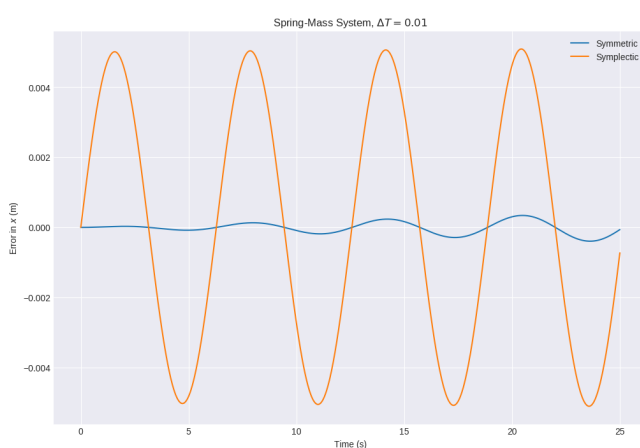




Spring-Mass system, $\Delta T = 0.01s$



Spring-Mass system, $\Delta T = 0.001s$



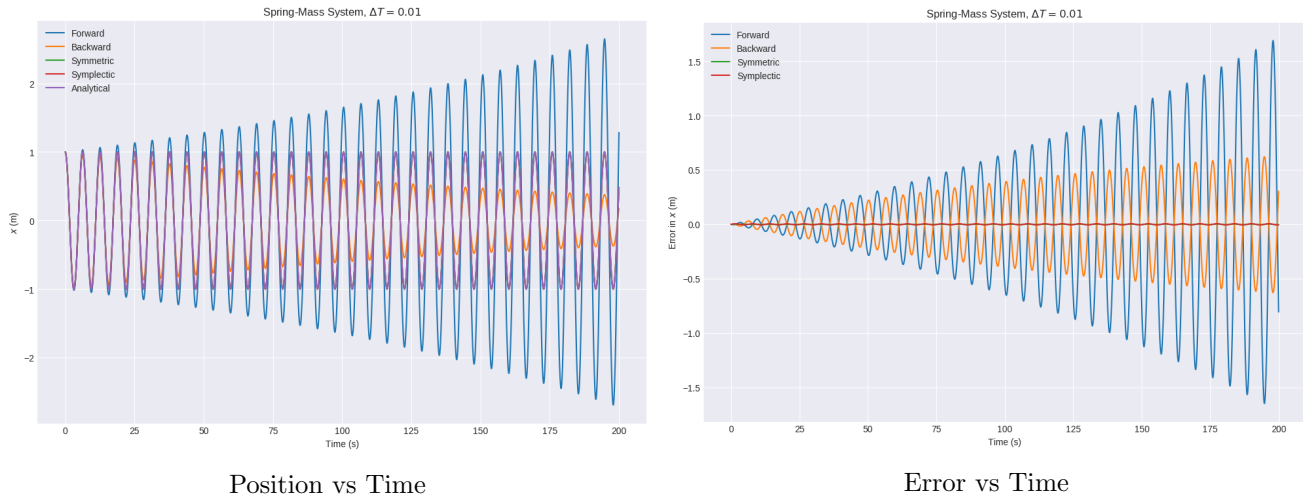
Error of Symplectic and Symmetric Euler

Spring-Mass system : Analysis with varying time horizon

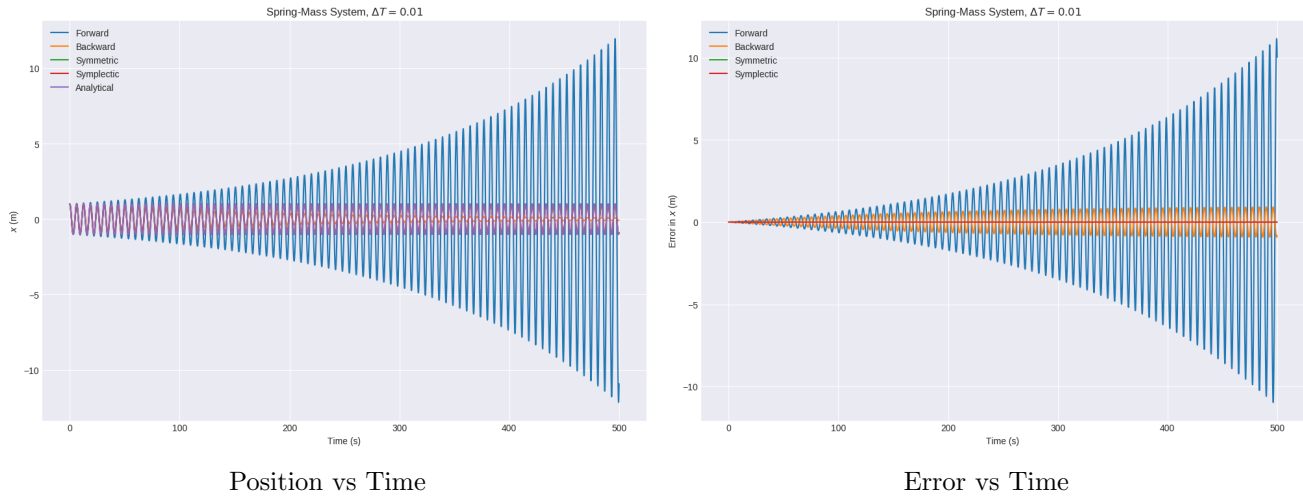
Variation of **absolute average error (in metres)** with horizon

Horizon (s)	Forward	Backward	Symmetric	Symplectic
200	0.4556	0.2336	0.0011	0.0035
500	2.2141	0.4031	0.0026	0.0038
1000	18.1593	0.5104	0.0053	0.0045

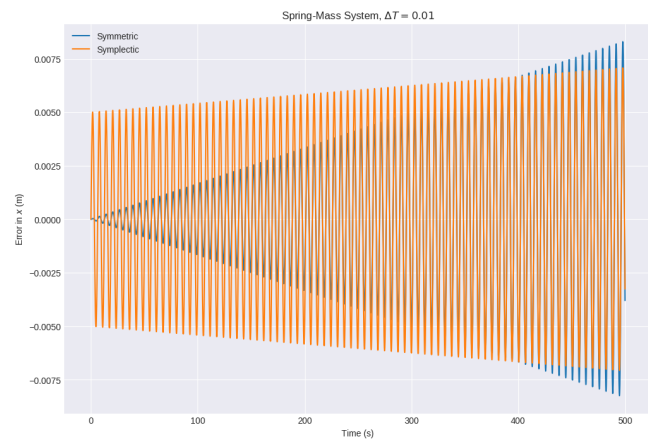
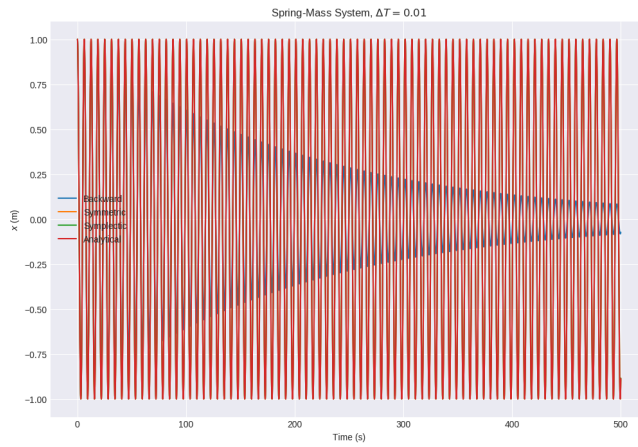
Forward and **Backward Euler** perform very poorly for large horizons. The error due of **Symmetric Euler** solution is lower than that of **Symplectic Euler** initially but it grows at a faster rate and Symplectic Euler performs better at larger horizons. For the given system, $\ddot{x} + x = 0$, all the numerical solutions diverge with time.



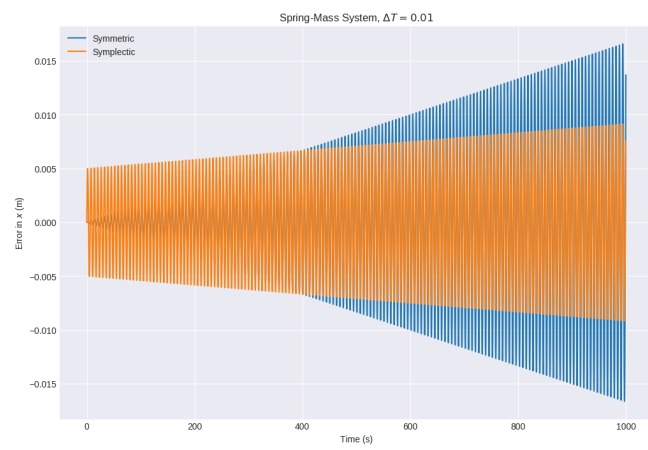
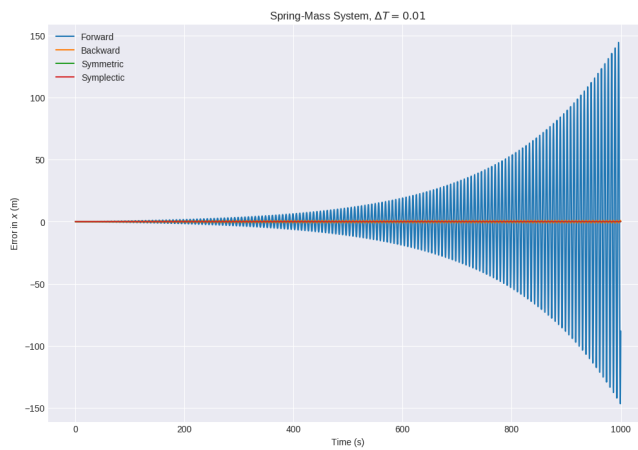
Spring-Mass system, Horizon= 200s



Spring-Mass system, Horizon= 500s

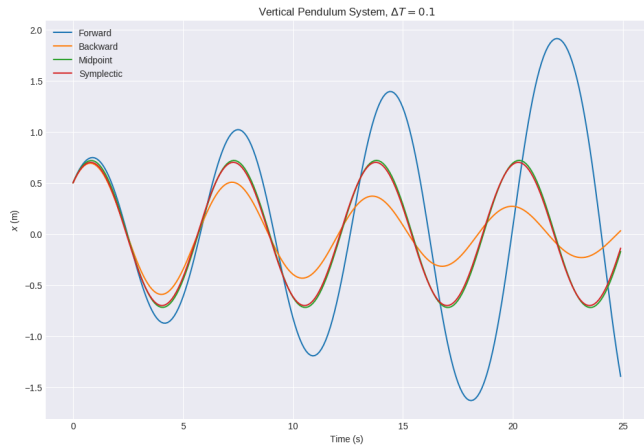


Spring-Mass system, Horizon= 500s

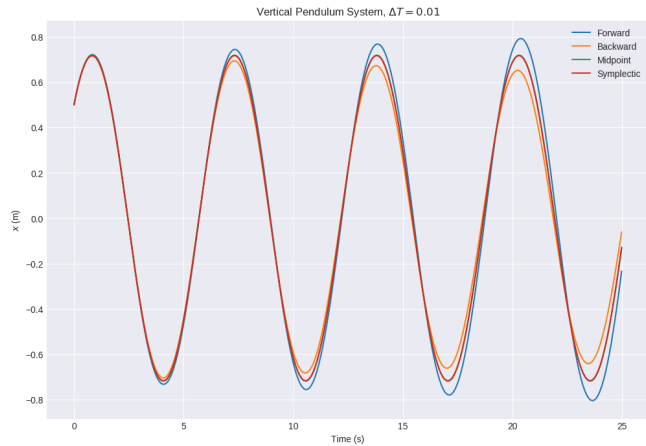


Spring-Mass system, Horizon= 1000s

Vertical Pendulum system

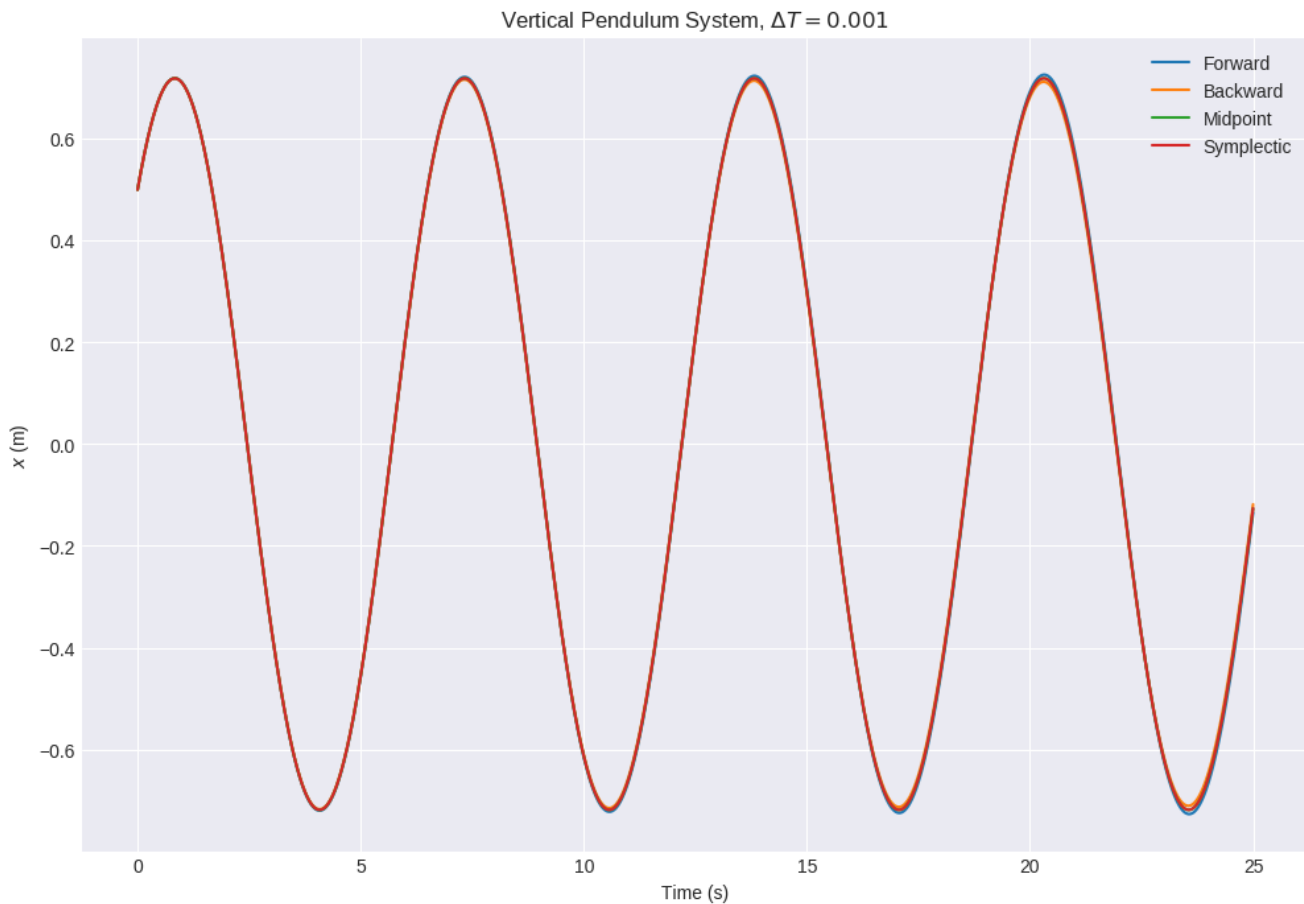


$\Delta T = 0.1s$

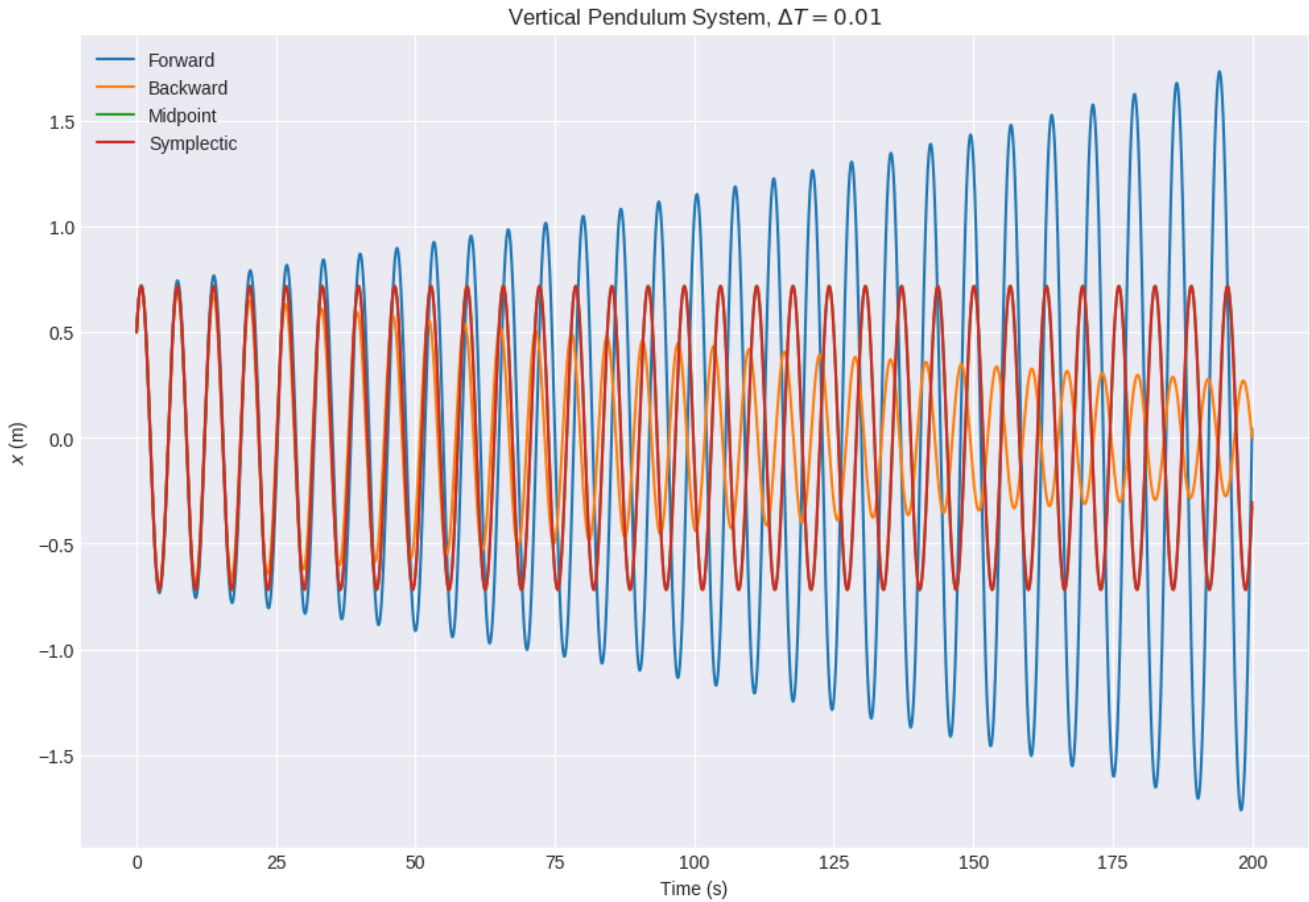


$\Delta T = 0.01s$

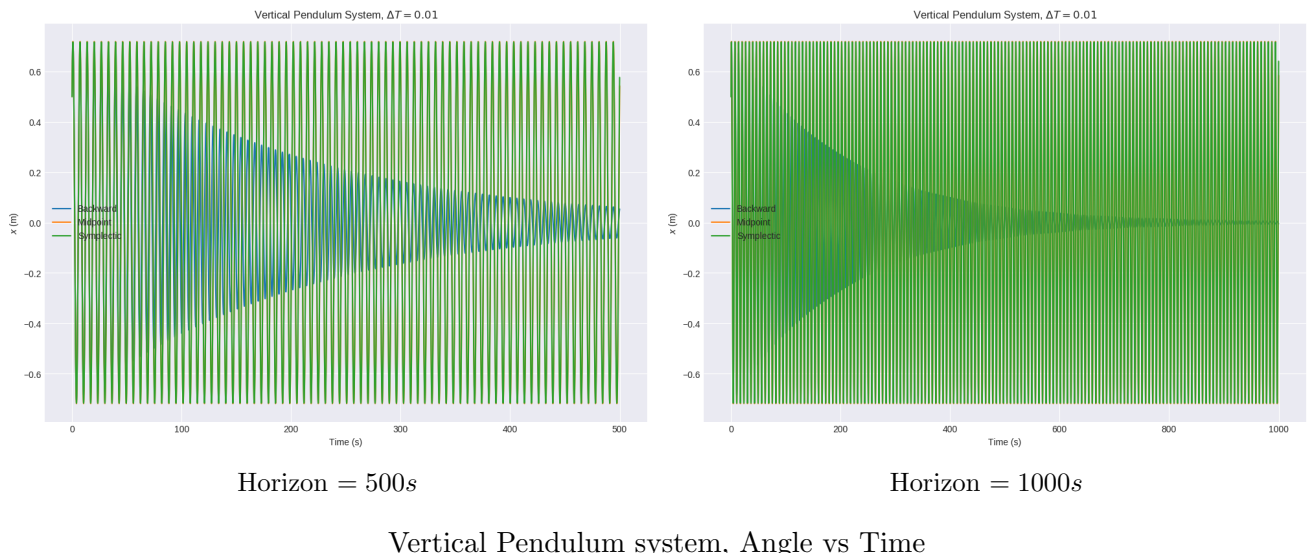
Vertical Pendulum system, Angle vs Time



Vertical Pendulum system, Angle vs Time



Vertical Pendulum system, Angle vs Time



The relative performances of the numerical methods is the same for even the pendulum system. Forward and Backward Euler quickly move away from the expected sinusoidal solution. This does not happen with Symmetric and Symplectic Euler.

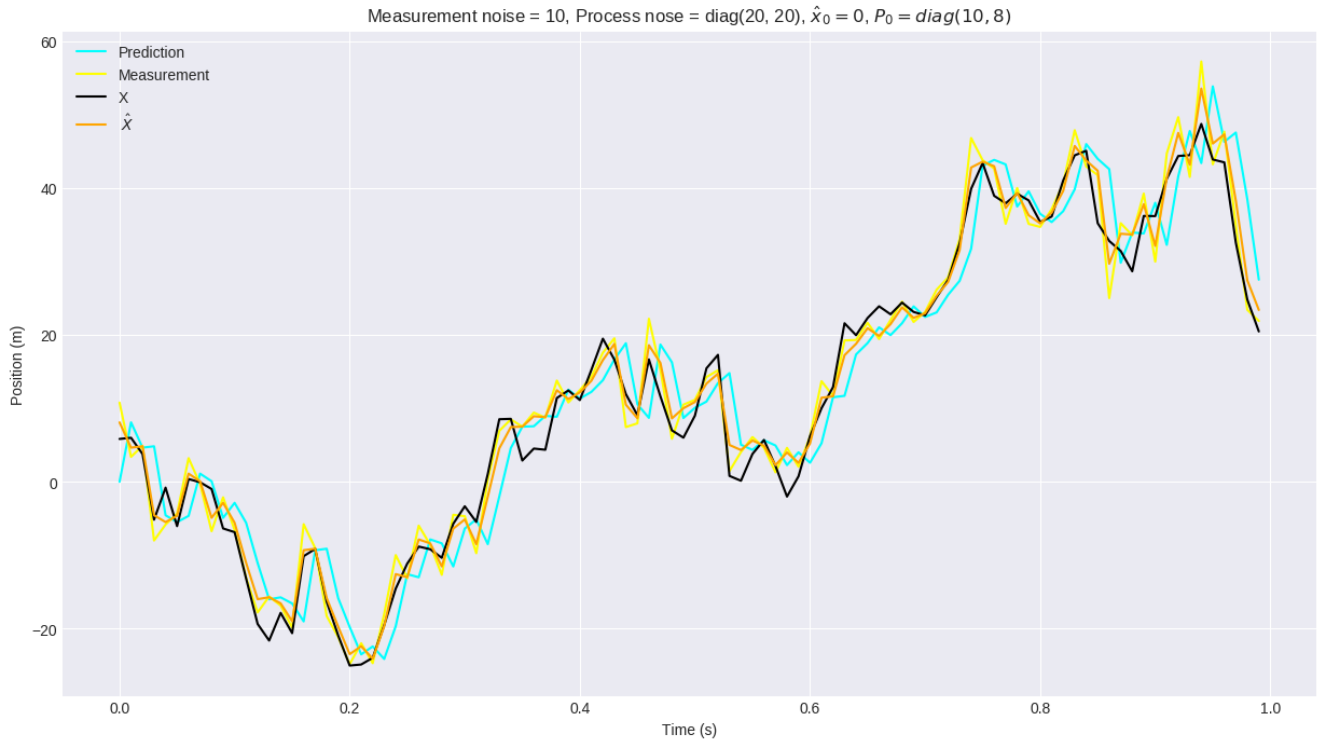
2 Kalman Filter

I simulated the following discrete dynamical system,

$$\mathbf{x}_{k+1} = F\mathbf{x}_k + w_k, \quad w_k \sim \mathcal{N}(\mathbf{0}, Q)$$

$$\mathbf{y}_k = H\mathbf{x}_k + v_k, \quad v_k \sim \mathcal{N}(\mathbf{0}, R)$$

Where $F = \begin{pmatrix} 1 & \Delta T \\ 0 & 1 \end{pmatrix}$, $H = (1 \ 0)$ and $\mathbf{x}_k = \begin{bmatrix} x \\ \dot{x} \end{bmatrix}$. For the simulation, I used $\Delta T = 0.01s$, $Q = \begin{pmatrix} 20 & 0 \\ 0 & 20 \end{pmatrix}$, $R = (10)$. The plots mention the parameters used by the **Kalman filter**.



Kalman filter

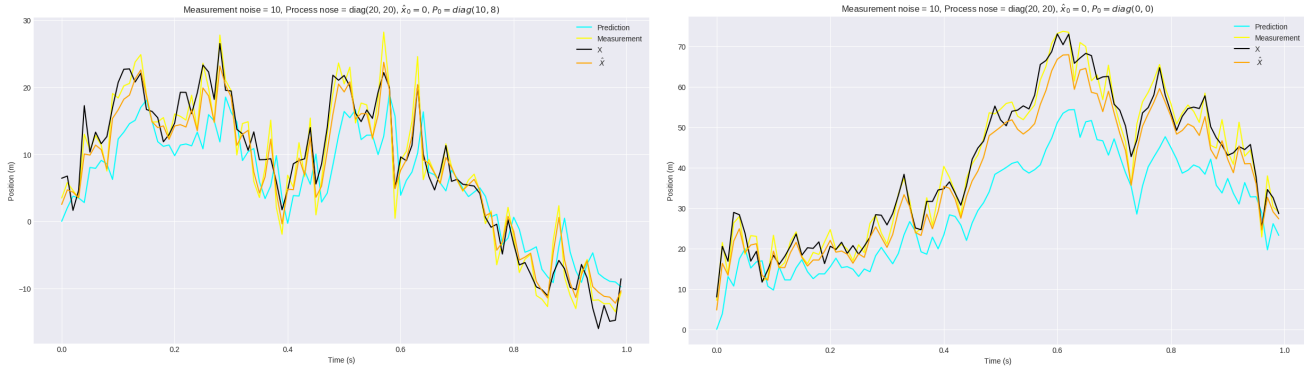
The above plot is an ideal situation when the model noise covariances and state-transition, measurement matrices are same as that of the original system. The estimate is close to the true value of the position of the cart.

However in a more realistic situation, the system matrices used in our model will be inaccurate and the noise covariances cannot be determined exactly. The filter still turns out to be robust enough to perform well under these circumstances. It can be seen from the graph below that model uncertainties lead to the prediction deviating from the true value of x but the Filter estimates are still close to the true value.

It is clearly noticeable how the Filter responds to changes in the Q and R matrices. Increasing the process-noise covariance causes the estimate to lie closer to the measurements and vice-versa.

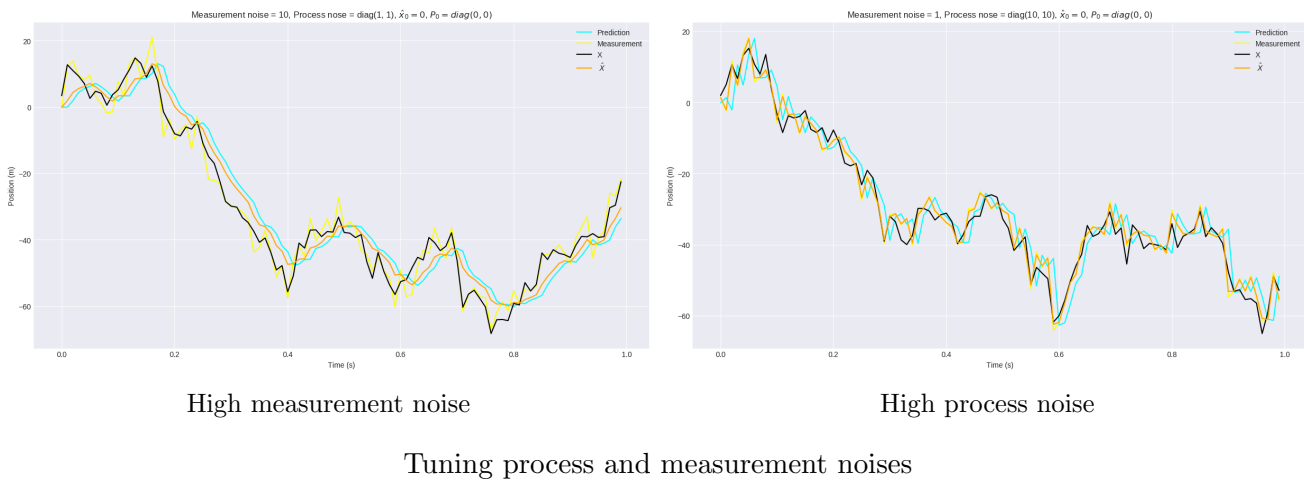
The Filter also recovers from large initial uncertainties quickly as can be seen in the graph below.

Uncertainty in the model

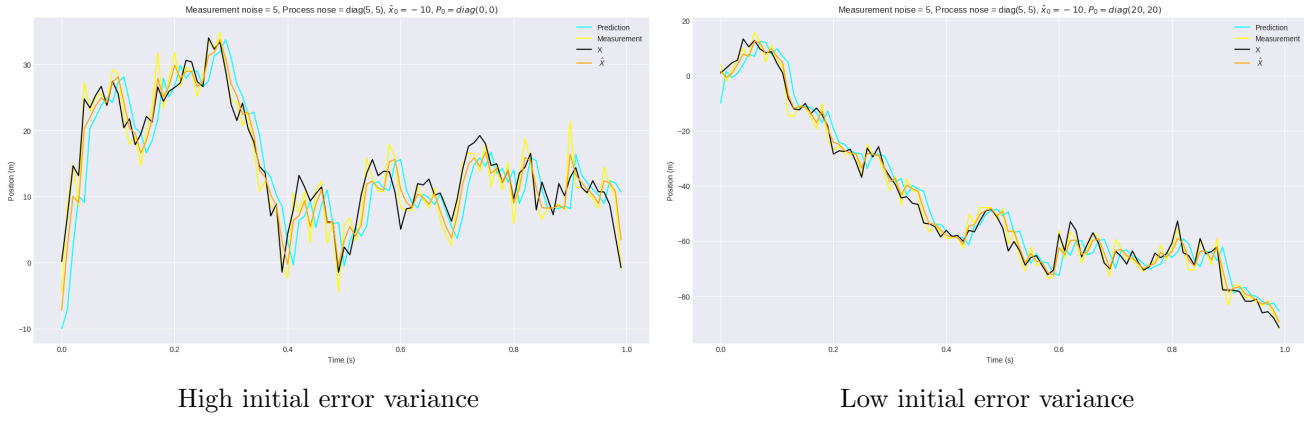


Uncertain model for two different initial error covariances

Tuning the covariances



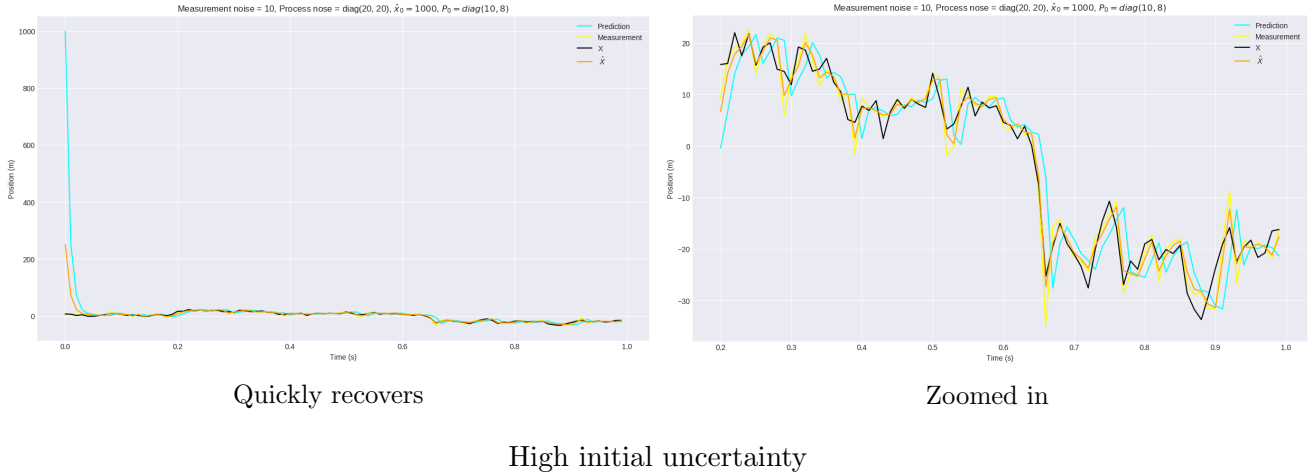
Here it is evident that for a high value of the measurement noise variance set in the filter, the estimate is closer to the prediction. Similarly for high values of process noise variance, the estimate is closer to the measurement.



Tuning initial state covariance

When the initial error covariance is low, the filter trusts the initial value of x_0 more and thus takes more time to converge to the true value as can be seen from the graph.

Large initial state uncertainty



3 Observer for linear dynamical system

We keep a proxy of the system along with the state \hat{x} and update it according to our model of the system and also a correction term as shown below.

$$\dot{x} = Ax \quad (1)$$

$$y = Cx \quad (2)$$

$$\dot{\hat{x}} = A\hat{x} + L(y - C\hat{x}) \quad (3)$$

Equations (1) and (2) represent the true system and (3) is our model of the system, where $L(y - C\hat{x})$ is the correction term. \hat{x} is our estimate for x and we can show that \hat{x} converges to x in the following manner,

$$\dot{\hat{x}} = A\hat{x} + LC(x - \hat{x}) \quad (4)$$

We get (4) by substituting (2) in (3). Now subtract (4) from (1) and define $e \triangleq x - \hat{x}$

$$\dot{e} = (A - LC)e \quad (5)$$

If (A, C) pair is controllable, we can choose an L such that $(A - LC)$ is Hurwitz.